

See discussions, stats, and author profiles for this publication at: <https://www.researchgate.net/publication/263948357>

Scaling Equations for Oil/Gas Recovery from Fractured Porous Media by Counter-Current Spontaneous Imbibition: From Development to Application

ARTICLE *in* ENERGY & FUELS · JULY 2013

Impact Factor: 2.79 · DOI: 10.1021/ef400990p

CITATIONS

12

READS

32

2 AUTHORS:



[Abouzar mirzaei paiaman](#)

34 PUBLICATIONS **95** CITATIONS

SEE PROFILE



[Mohsen Masihi](#)

Sharif University of Technology

115 PUBLICATIONS **407** CITATIONS

SEE PROFILE

Scaling Equations for Oil/Gas Recovery from Fractured Porous Media by Counter-Current Spontaneous Imbibition: From Development to Application

Abouzar Mirzaei-Paiaman and Mohsen Masihi*

Department of Chemical and Petroleum Engineering, Sharif University of Technology, P.O. Box 11365-9465, Tehran, Iran

ABSTRACT: Spontaneous imbibition, the capillary-driven process of displacing the nonwetting phase by the wetting phase in porous media, is of great importance in oil/gas recovery from matrix blocks of fractured reservoirs. The question of how properly scaling up the recovery by counter-current spontaneous imbibition has been the subject of extensive research over decades, and numerous scaling equations have been proposed. As a convention, the scaling equations are usually defined analytically by relating the early time squared recovery to squared pore volume. We show this convention does not apply to common scaling practices and, if used, causes nontrivial scatter in the scaling plots. We explain that for three common scaling practices, where the recovery is normalized by (1) final recovery, (2) pore volume, or (3) initial oil/gas in place, this convention should be redefined accordingly. The main contribution is to emphasize that during the development of any scaling equation, its consistency with common applications should be considered. Such consistency has been historically neglected in literature works. Using this new insight, we consider the latest scaling published in the literature to present three different consistent scaling equations for three corresponding scaling situations. The new scaling equations, which are valid for both gas–liquid and liquid–liquid systems, incorporate all factors influencing the process and resolve all limitations of scaling groups published during past decades. These scaling equations are rewritten in terms of two physically meaningful dimensionless numbers, $Da^{1/2}/Ca$ (Da , Darcy number; Ca , capillary number), and validated against experimental data from the literature. This approach enables us to scale all data perfectly and represents all recovery curves by a single master curve. We further highlight the necessity of incorporation of directional permeability effects in scaling equations by defining the new concept of characteristic permeability.

1. INTRODUCTION

Fractured reservoirs host a significant portion of the world's petroleum reserves and are often considered to be composed of two distinct media: a medium of highly permeable and low storage volume fractures and a medium of a less permeable and high storage volume rock matrix.¹ In such reservoirs, imbibition, the process of displacing the nonwetting phase (NWP) by the wetting phase (WP), is an important mechanism for oil/gas, NWP, recovery during aquifer invasion, water flooding, and in general any enhanced recovery method where an aqueous based fluid, WP, is injected into the fracture network.^{2–4} The aqueous based fluid when contacting the NWP saturated matrix blocks can imbibe from the surrounding fractures into the matrix blocks, if favorable conditions exist. One of the mechanisms responsible for production of the NWP from the matrix blocks can be counter-current spontaneous imbibition (COUCSI) where capillary forces are the only driving forces for the displacement and the two phases are flowing in the opposite direction. This process is also of great importance in many of other applications including wettability evaluation of reservoir rocks,⁵ brine intake potential and wettability evaluation of organic shales,^{6,7} formation damage through aqueous phase trapping in tight gas reservoirs,^{8–10} and steam migration in geothermal formations.¹¹

An important challenge that has been the focus of research for decades is how to scale the NWP recovery by COUCSI. In scaling practices, usually the recovery curves normalized by a reference volume (i.e., the pore volume, the initial NWP in place, or the ultimate recovery) are plotted versus a scaling time

group (or dimensionless time). The first scaling equation published addressing this issue was the classical work by Rapoport.¹² Rapoport presented the scaling criteria for two-phase incompressible immiscible flow through porous media. Using inspectional analysis of the differential equations of WP/NWP flow through porous media, he found that the saturation distribution was a function of dimensionless time provided some certain similarities were presented. This dimensionless time describes how NWP recovery can be estimated in systems with different properties because the recovery in both systems at homologous times should be the same. According to Rapoport's scaling analysis under proper conditions of scaling, homologous times should correspond to equal cumulative recoveries between two systems (i.e., model and prototype). On the basis of the work by Rapoport,¹² Mattax and Kyte¹³ presented a scaling equation for scaling COUCSI. However, they neglected the fact that Rapoport did not distinguish between different lengths (see Rapoport's eq 17), which, as will be presented later, results in the condition of equal squared recoveries between model and prototype.

Besides the inconsistency associated with the scaling group of Mattax and Kyte,¹³ some restrictive assumptions were used to derive this scaling equation. These assumptions were that the shape of the model must be identical to that of the prototype, the prototype WP to NWP viscosity ratio must be duplicated in

Received: May 25, 2013

Revised: July 8, 2013

Published: July 9, 2013

Table 1. Summary of Different Scaling Equations Proposed Sequentially by Rapoport,¹² Mattax and Kyte,¹³ Kazemi et al.,¹⁵ and Ma et al.,¹⁶ As Well As Different Shape Factors

reference	scaling equation (dimensionless time)	shape factor	definitions
Rapoport ¹²	$t_{D,R} = \frac{k \frac{dp_c}{ds_w}}{u \mu_w L}$		$t_{D,R}$ is the dimensionless time due to Rapoport; k , the absolute permeability; u , the volumetric flux or Darcy velocity; μ_w , the WP viscosity; P_c , the capillary pressure; L , the length of the matrix block; and S_{w0} the saturation of WP
Mattax and Kyte ¹³	$t_{D,MK} = \frac{\sigma \sqrt{\frac{k}{\phi}}}{\mu_w L^2} t$		$t_{D,MK}$ is the dimensionless time due to Mattax and Kyte; σ , the interfacial tension; ϕ , the porosity, and t , the time
Kazemi et al. ¹⁵	$t_{D,KGE} = \frac{\sigma \sqrt{\frac{k}{\phi}} F_{s,KGE}}{\mu_w} t$	$F_{s,KGE} = \frac{1}{V_{ma}} \sum_{i=1}^s \frac{A_{ma,i}}{d_{ma,i}}$	$t_{D,KGE}$ and $F_{s,KGE}$ are, respectively, the dimensionless time and shape factors due to Kazemi, Gilman, and Elsharkawy; s , the number of the open faces to imbibition; V_{ma} , the matrix bulk volume; $A_{ma,i}$, the area of a surface area open to flow in a given flow direction; and $d_{ma,i}$, the distance from the open surface to the center of the matrix block
Ma et al. ¹⁶	$t_{D,MZM} = \frac{\sigma \sqrt{\frac{k}{\phi}} F_{s,MZM}}{\mu_w} t$	$F_{s,MZM} = \frac{1}{V_{ma}} \sum_{i=1}^s \frac{A_{ma,i}}{l_{ma,i}} = \frac{1}{L_c^2}$	$t_{D,MZM}$ and $F_{s,MZM}$ are, respectively, the dimensionless time and shape factors due to Ma, Zhang, and Morrow; l_{ma} , the distance from the open surface to the no-flow boundary; and L_c , the characteristic length

the model tests, initial fluid saturations in the prototype and the pattern of WP movement in the surrounding fractures must be duplicated in the model tests, the relative permeability functions must be the same for both the model and the prototype, and finally the capillary pressure functions for the both the model and the prototype must be related by direct proportionality. To remove some of these constraints, several studies attempted to present improvements to the scaling equation of Mattax and Kyte,¹³ but still lacking the aforementioned consistency.

Based on theoretical works by Warren and Root¹ and Kazemi et al.¹⁴ on the simulation of WP-NWP displacement in fractured reservoirs, Kazemi et al.¹⁵ proposed a shape factor to account for the effects of different sample size, shape, and boundary conditions on spontaneous imbibition. They added the term shape factor to the scaling equation previously proposed by Mattax and Kyte¹³ and suggested using their own scaling equation. Ma et al.¹⁶ by looking at physical considerations of the COUCSI process proposed a modified form of shape factor and defined the characteristic length in the scaling equation. The core length in scaling equation of Mattax and Kyte¹³ when replaced by characteristic length as defined by Ma et al.¹⁶ is expected to account for the effect of different sample size, shape, and boundary conditions on COUCSI. Many authors showed the validity of the characteristic length formula, by using the experimental data.^{17–23} It is emphasized that the characteristic length has been derived analytically, by using classical formulations of two-phase flow in porous media, for some geometrical shapes by Mason et al.²⁴ Heinemann and Mittermeir²⁵ derived the shape factor using control volume finite difference discretization on the fracture-matrix dual continuum. On the basis of this derivation, they concluded that this shape factor was exact under pseudo-steady-state conditions within the dual continuum mathematical concept of natural fractured dual porosity systems. Table 1 summarizes various scaling equations, shape factors, and characteristic length.

To properly account for the effect of phase viscosity in scaling equations, many works have been conducted. Gupta and Civan²⁶ and Behbahani and Blunt²⁷ used the WP viscosity term in their scaling equations, while Iffly et al.,²⁸ Cuiec et al.,²⁹ and Babadagli³⁰ used NWP viscosity instead of WP viscosity. Ma et al.¹⁶ experimentally observed that the imbibition time was proportional to the geometric mean of WP and NWP viscosities. Therefore, they used the term of geometric mean instead of WP viscosity. Wang³¹ proposed another form of viscosity. However, the use of this form and also the geometric mean does not respond when the viscosity of NWP becomes

relatively small (as with air, or with a highly viscous WP, for example).^{17,20,21,23,32} To resolve this problem, Fischer et al.²¹ and Mason et al.²³ proposed their own forms. Table 2 contains different forms of viscosity used in literature works.

Table 2. Summary of Different Viscosity Terms Used in Literature Works to Account for Phase Viscosity Effects

reference	phase viscosity term	definitions
Mattax and Kyte, ¹³ Gupta and Civan, ²⁶ and Behbahani and Blunt ²⁷	μ_w	
Iffly et al., ²⁸ Cuiec et al., ²⁹ and Babadagli ³⁰	μ_{nw}	μ_{nw} is the NWP viscosity
Ma et al. ¹⁶	$\sqrt{\mu_w \mu_{nw}}$	
Wang ³¹	$\mu_w^{0.75} \mu_{nw}^{0.25}$	
Fischer et al. ²¹	$\frac{a \cdot b}{\mu_w + b^2 \mu_{nw}}$	a and b are two fitting parameters
Mason et al. ²³	$\mu_w + \sqrt{\mu_w \mu_{nw}}$	

Other constraints in scaling equations are represented by parameters which are highly controlled by the system wettability, namely initial fluid saturations, relative permeability, and capillary pressure functions. If these parameters are excluded from the scaling equation, then it will be able to scale only systems with the same wettability at best. But spontaneous imbibition can occur in a variety of wetting conditions such as strongly water-wet (SWW), weakly water-wet (WWW), mixed-wet (MW), and fractional-wet (FW) states of rock, each with different extents.³³ To account for different wettability effects, Iffly et al.²⁸ and Gupta and Civan²⁶ added empirically the term cosine of the contact angle to the base scaling equation. However, it is generally accepted that in the case of petroleum bearing rocks, assigning a single value for contact angle is impractical.³³ The contact angle, for example, cannot take into account the roughness, heterogeneity, and complex geometry of reservoir rocks. Reservoir rocks are complex structures, often comprising a variety of mineral types. Each mineral may have a different wettability, making the wetting character of the composite rock difficult to describe using a simple contact angle measurement. In another work, the linear relationship between the NWP recovery versus the square root of time was used.³⁴ Babadagli³⁰ inferred that the slope of such plots is only a function of wettability if all other parameters are held constant. He conducted a set of experiments using the same rock and fluid system but with different wettability conditions and developed an index for quantifying the wettability effects. He used this index as a new term in the

base scaling equation. Pordel Shahri et al.³⁵ proposed another normalization index of this type.

Another matter, not usually discussed in the previous scaling works, is that Rapoport¹² presented his scaling criteria for systems in which the intrinsic permeability was the same in all directions of the matrix block. Therefore, in the scaling equations published so far, the same assumption has been used considering permeability measured in only one direction (i.e., direction where forced displacement is implemented in the flood experiments). But in practice, there exist several possible boundary conditions for counter-current flow. For example, for a cylindrical matrix block, several different boundary conditions of counter-current flow experiments could be simulated in which in all cases the open face(s) is the reservoir of WP and this face(s) hosts the production of NWP, as well. These cases are one end open (one-dimensional linear flow), two ends open (one-dimensional linear flow), two ends closed (two-dimensional radial flow), one end closed (three-dimensional linear and radial flows), and all faces open (three-dimensional linear and radial flows). Obviously, for situations where the flow is not one-dimensional (i.e., two- or three-dimensional), it seems crucial to account for the variation in directional permeability within the matrix block, which also affects the relative permeability and capillary pressure functions. It is therefore necessary to include the effect of variation in permeability, relative permeability, and capillary pressure in different directions into the scaling equations, just as Kazemi et al.¹⁵ and Ma et al.¹⁶ did for different boundary conditions. However, unlike the permeability which is usually measured in more than one direction, measurement of relative permeability and capillary pressure in different directions is not common. For the case of permeability in different directions, the new concept of characteristic permeability k_c may be defined using the geometric mean of permeability values using eq 1. The permeability term in scaling equations may therefore be substituted by the characteristic permeability term to account for permeability in each direction.

$$k_c = \left(\prod_{j=1}^n k_j \right)^{1/n} \quad (1)$$

in which n is the total number of flow directions. The subject of accounting for the directional relative permeability and capillary pressure in scaling equations remains open for future works.

Most of the available scaling equations are based on the scaling equation proposed by Mattax and Kyte¹³ itself based on the inspectional analysis performed by Rapoport.¹² The second methodology exists by which the scaling equations are derived mathematically using the standard analysis of one-dimensional two-phase flow in porous media. The scaling equations of the second methodology do have the same structural form as the scaling equations of the first methodology. The standard analysis combines the Darcy equation for both phases with the continuity equation for WP, capillary pressure definition, and the condition of COUCSI (the total velocity equals to zero). The resulting equation will be a highly nonlinear parabolic partial differential equation of second order. Several authors have used approximate solutions to this equation to propose scaling equations.^{21,22,24,36–42} They use some assumptions. They, for example, assume capillary pressure and relative permeability functions to be constant and evaluated at some specific saturations, e.g., constant capillary pressure and relative permeability at the end point saturations. Among them, the assumptions made by Reis and Cil,³⁶ Li and Horne,⁴⁰ Li,⁴¹

Fischer et al.,²¹ and Mason et al.^{22,24} are restricting since they take the assumption of a linear capillary pressure profile and constant capillary pressure derivative, i.e., piston-like displacement. This assumption is based on the experimental results for gas–liquid systems, where the saturation profile often is piston-like.³⁴ Recently, Schmid et al.⁴³ made the observation that the McWhorter and Sunada⁴⁴ analytical solution is applicable to COUCSI without the use of artificial boundary conditions. Schmid and Geiger⁴⁵ used this exact solution and introduced a scaling equation applicable for SWW systems. They later extended their approach to account for the wettability effects.⁴⁶ However, the main flaw of the scaling equations of the second category is that they do not consider the consistency between the development of scaling equations and common applications. In scaling practices, usually the recovery curves normalized by a reference volume (i.e., the pore volume, the initial NWP in place, or the ultimate recovery) are plotted versus a scaling group. They, however, as a convention define their scaling equations by relating the squared recovery to the squared pore volume. We believe and show that this blind convention does not apply for common scaling practices and, if used, results in nontrivial scatter in scaling results.

In this paper, emphasis will be put on the requirements that analytically derived scaling expressions should obey according to common scaling practices in order to generate consistent plots for the normalized NWP recovery versus the scaling time. For this purpose, we first modify the analysis of Rapoport¹² and show that the early well-known scaling equation of Mattax and Kyte¹³ and subsequent scaling equations, for which attempts were made to define them as having the same structural form as the original, correspond to equal but squared recoveries between two systems. We then explain that for three common scaling practices, where the recovery normalized by either final recovery, pore volume, or initial oil in place is usually placed on the vertical axis of scaling plots, the classical blind convention should be redefined accordingly. We consider the latest scaling work in the literature to present three different consistent scaling equations for three corresponding scaling situations. We show that these scaling equations are physically meaningful and can be expressed in terms of two dimensionless numbers as $Da^{1/2}/Ca$ (Da , Darcy number; Ca , capillary number). The new scaling equations are then validated against experimental data from the literature. Finally, conclusions will be drawn from this work.

2. DERIVATION OF SCALING EQUATION OF MATTAX AND KYTE¹³ FROM MODIFIED ANALYSIS OF RAPOPORT¹²

In this section, we follow the derivation for the scaling equation of Mattax and Kyte¹³ and show that it is not consistent to common scaling practices. Basically, we use the formulations of Rapoport,¹² but the current approach differs from that of Rapoport in the way that he assumed a single term L for all lengths but we distinguish between different lengths.

For the one-dimensional isothermal immiscible flow of two incompressible fluids in the porous medium with only one face open to flow (i.e., counter-current flow), neglecting gravity effects, as well as nonequilibrium effects,^{45–47} combining Darcy's law for WP and NWP, the capillary pressure definition, and the mass continuity equation for the WP gives^{45,46}

$$\phi \frac{\partial S_w}{\partial t} = \frac{\partial}{\partial x} \left(D(S_w) \frac{\partial S_w}{\partial x} \right) \quad (2)$$

in which x is the coordinate distance and $D(S_w)$, the capillary diffusion function defined as

$$D(S_w) = -f(S_w)k_{rnw} \frac{dP_c}{\mu_{nw} dS_w} \quad (3)$$

and k_{rnw} is the counter-current relative permeability of NWP and $f(S_w)$, the fractional flow function defined as

$$f(S_w) = \frac{k_{rw}\mu_{nw}}{k_{rw}\mu_{nw} + k_{rnw}\mu_w} \quad (4)$$

in which k_{rw} is the counter-current relative permeability of WP. Inserting eq 3 into eq 2 gives

$$\phi \frac{\partial S_w}{\partial t} + \frac{k}{\mu_{nw}} \frac{\partial}{\partial x} \left(k_{rnw} f(S_w) \frac{dP_c}{dS_w} \frac{\partial S_w}{\partial x} \right) = 0 \quad (5)$$

Equation 5, written for the model, can be used once again but for the prototype, as was used in Rapoport:¹²

$$\phi' \frac{\partial S_w}{\partial t'} + \frac{k'}{\mu_{nw}'} \frac{\partial}{\partial x'} \left(k_{rnw} f(S_w) \frac{dP_c'}{dS_w} \frac{\partial S_w}{\partial x'} \right) = 0 \quad (6)$$

where prime sign “'” differentiates between model and prototype parameters. For the sake of simplicity, we have assumed the same values of $k_{rnw}f(S_w)$ between the model and prototype, as Rapoport¹² did too.

Just the same as Rapoport,¹² we define the ratios of model to prototype parameters as $\phi/\phi' = C$, $k/k' = D$, $\mu/\mu_w' = \mu/\mu_{nw}' = F$, $[(dP_c)/(dS_w)]/[(dP_c')/(dS_w)] = G$, and $(q_w)/(q_w') = B$, in which q_w is the volumetric flow rate. But unlike Rapoport, we distinguish between different lengths (i.e., system length and distance to the front) and define $x/x' = N$ and $W/W' = P$, in which W is the cross-section width of the core perpendicular to the flow direction. Therefore, one can write¹²

$$\frac{u_w}{u_w'} = \frac{\frac{q_w}{W^2}}{\frac{q_w'}{W'^2}} = \frac{B}{P^2} \quad (7)$$

in which u_w is the volumetric flux or Darcy velocity of the WP. As will be shown later, the Darcy velocity u_w can be related to linear velocity v_w as

$$u_w = \frac{v_w \phi}{F'(S_{wi})} \quad (8)$$

where S_{wi} is the initial saturation of WP and $F'(S_{wi})$ will be discussed later. It should be noted that in eq 8, $\phi/[F'(S_{wi})]$ is the fraction of the pore volume available for WP to flow across. Just for the sake of simplicity, we assume that $F'(S_{wi})$ is the same between the model and prototype, as we did before for $k_{rnw}f(S_w)$.

Using eq 8 and applying the established definitions between model and prototype parameters, we can write

$$\frac{t}{t'} = \frac{\frac{x}{v_w}}{\frac{x'}{v_w'}} = \frac{\frac{x}{u_w}}{\frac{x'}{u_w'}} = \frac{NCP^2}{B} \quad (9)$$

As a result, using eq 9 we can write

$$\frac{\partial S_w}{\partial t} = \frac{B}{NCP^2} \frac{\partial S_w}{\partial t'} \quad (10)$$

Using the above definitions, then eq 5 can be rewritten as

$$\phi' \frac{\partial S_w}{\partial t'} + \frac{P^2GD}{BNF} \frac{k'}{\mu_{nw}'} \frac{\partial}{\partial x'} \left(k_{rnw} f(S_w) \frac{dP_c'}{dS_w} \frac{\partial S_w}{\partial x'} \right) = 0 \quad (11)$$

Bringing eq 11 (i.e., the governing equation for the model) and eq 6 (i.e., the governing equation for the prototype) equal gives

$$\frac{P^2GD}{BNF} = 1 \quad (12)$$

Equation 12 is the necessary condition to have the equal recoveries between model and prototype, because to arrive at this equation, governing equations for the model, with a solution of $S_w(x,t)$, and prototype, with a solution of $S_w(x',t')$, were brought equal. Using the previously defined ratios, then this equation can be rewritten as

$$\frac{k}{u_w \mu_{nw} x} \frac{dP_c}{dS_w} = \frac{k'}{u_w' \mu_{nw}' x'} \frac{dP_c'}{dS_w} \quad (13)$$

The relationship between capillary pressure and Leverett J function $J(S_w)$ can be expressed as:⁴⁸

$$P_c(S_w) = \sigma \sqrt{\frac{\phi}{k}} J(S_w) \quad (14)$$

Inserting eqs 8 and 14 into eq 13 and assuming $(dJ)/(dS_w) = (dJ')/(dS_w)$ gives

$$\frac{\sigma \sqrt{\frac{k}{\phi}}}{v_w \mu_{nw} x} = \frac{\sigma' \sqrt{\frac{k'}{\phi'}}}{v_w' \mu_{nw}' x'} \quad (15)$$

Multiplying both sides of eq 15 by xx' and then dividing both sides by LL' , this equation can be rewritten as

$$\frac{\frac{Da^{1/2}}{Ca}}{\frac{Da^{1/2}}{Ca'}} = \frac{\frac{\sigma \sqrt{\frac{k}{\phi}}}{v_w \mu_{nw} L}}{\frac{\sigma' \sqrt{\frac{k'}{\phi'}}}{v_w' \mu_{nw}' L'}} = \frac{\frac{x}{L}}{\frac{x'}{L'}} = \frac{\frac{Q}{Q_\infty}}{\frac{Q'}{Q_\infty'}} \quad (16)$$

where, as will be shown later,

$$\frac{Q}{Q_\infty} = \frac{F'(S_{wi}) x}{F'(S_w) L} \quad (17)$$

where Q is the cumulative volumetric recovery at any time and Q_∞ is the final cumulative recovery where the imbibition front hits the no-flow boundary. Just for the sake of simplicity, we assume that $F'(S_w)$ is the same between the model and prototype, as we did before for $F'(S_{wi})$, $J(S_w)$, and $k_{rnw}f(S_w)$. In eq 16, Da and Ca are, respectively, two dimensionless numbers, Darcy number⁴⁹ and Capillary number,⁵⁰ defined as

$$Da = \frac{k}{\phi L^2} \quad (18)$$

$$Ca = \frac{v_w \mu_{nw}}{\sigma} \quad (19)$$

Equation 16 shows that a consistent scaling group derived from relating the homologous times to equal recoveries between the model and prototype should have the form of $Da^{1/2}/Ca$. In eq 16, when substituting v_w by x/t and v_w' by x'/t' , a simple manipulation gives

$$\frac{\frac{Da}{Ca^2}}{\frac{Da'}{Ca'^2}} = \frac{\frac{\sigma \sqrt{\frac{k}{\phi}}}{\mu_{nw} L^2} t}{\frac{\sigma' \sqrt{\frac{k'}{\phi'}}}{\mu_{nw}' L'^2} t'} = \left(\frac{x}{L} \right)^2 = \left(\frac{Q}{Q_\infty} \right)^2 \quad (20)$$

It should be noted that in eq 20 either μ_{nw} or μ_w may be used because of the ratio defined before (i.e., $\mu_w/\mu_w' = \mu_{nw}/\mu_{nw}'$). Therefore, eq 20 clearly shows that the scaling group of Mattax and Kyte¹³ represents the situation where this dimensionless time is corresponding to equal squared recoveries between the model and prototype, this is while, in common scaling practices, as a general criterion, usually the normalized recovery is plotted versus the scaling equation. Therefore, $t_{D,MK}$ having the form of Da/Ca^2 is not according to general scaling criteria, which says a consistent scaling group should have the form of $Da^{1/2}/Ca$. This inconsistency can be found in other scaling equations, as well. Furthermore, it can easily be shown that all scaling groups derived from the standard analysis of one-dimensional two-phase flow in porous media (e.g.,^{36,37,41,45,46}) have the same structural form as $t_{D,MK}$ (i.e., Da/Ca^2) and are different from the general scaling criterion. It should be noted that if one does not distinguish between different lengths, as Rapoport¹² and Mattax and Kyte¹³ did, then the scaling equation of Mattax and Kyte¹³ incorrectly corresponds to equal recoveries between two systems (i.e., model and prototype).

3. DEVELOPING CONSISTENT SCALING EQUATIONS FOR COUCSI BY USING REDEFINED CONVENTIONS

Schmid et al.⁴³ noticed that the McWhorter and Sunada⁴⁴ analytical solution to eq 2 is applicable to COUCSI without the use of artificial boundary conditions. Indeed, they showed that the imposed boundary condition, as will be defined later in eq 23, is redundant for COUCSI, and the solution describes the standard situation found in the laboratory.⁴³ McWhorter and Sunada⁴⁴ presented this solution using the method of McWhorter⁵¹ that made use of a fractional flow function. The initial and boundary conditions used are as given in eqs 21, 22, and 23.⁴⁴

$$S_w(x, 0) = S_{wi} \quad (21)$$

$$S_w(+\infty, t) = S_{wi} \quad (22)$$

$$u_w(0, t) = At^{-1/2} \quad (23)$$

In the inlet boundary condition equation, A is a positive parameter that depends on the characteristics of the fluid-rock system defined as⁴⁴

$$A = \sqrt{\frac{\phi}{2} \int_{S_{wi}}^{S_{w,BC}} \frac{(S_w - S_{wi})D(S_w)}{F(S_w)} dS_w} \quad (24)$$

in which $S_{w,BC}$ is the saturation of WP at the open boundary. In this equation, F is a fractional flow function defined as⁴⁴

$$F(S_w) = 1 - \frac{\int_{S_w}^{S_{w,BC}} \frac{(\beta - S_w)D(\beta)}{F(\beta)} d\beta}{\int_{S_{wi}}^{S_{w,BC}} \frac{(S_w - S_{wi})D(S_w)}{F(S_w)} dS_w} \quad (25)$$

The solution presented by McWhorter and Sunada is given by the inverse formula:⁴⁴

$$x(S_w, t) = \frac{2A}{\phi} F'(S_w) t^{1/2} \quad (26)$$

in which F' is the derivate of F with respect to S_w defined as⁴⁴

$$F'(S_w) = \frac{\int_{S_w}^{S_{w,BC}} \frac{D(\beta)}{F(\beta)} d\beta}{\int_{S_{wi}}^{S_{w,BC}} \frac{(S_w - S_{wi})D(S_w)}{F(S_w)} dS_w} \quad (27)$$

This solution could be used by first prescribing $S_{w,BC}$ and calculating F from eq 25 and finally computing A from eq 24. However, the use of eq 25 is indirect, as it has the form of an implicit functional equation, from which $F(S_w)$ has to be extracted; therefore, computation of $F(S_w)$ from the integral eq 25 is done by iteration. A convenient first trial is $F(S_w) = 1$.⁴⁴

Schmid and Geiger^{45,46} used the exact analytical solution of McWhorter and Sunada⁴⁴ to develop the latest scaling equation defined using the classical blind convention by relating the squared recovery to squared pore volume. Our results presented later in section 4 show that this convention does not apply for common applications. In the following discussion, their approach and formulations are used to find the scaling equations consistent with the common scaling practices by using accordingly redefined conventions. Later, their scaling equation will be presented as well. Equation 23 can be integrated to yield the cumulative volumetric recovery at any time Q as

$$Q = S \int_0^t u_w dt = 2Sat^{1/2} \quad (28)$$

in which S is the surface area perpendicular to flow direction. Similarly the ultimate cumulative volumetric recovery Q_∞ , defined as the cumulative recovery up to the time at which the imbibition front hits the no flow boundary, can be derived as

$$Q_\infty = S \int_0^{t^*} u_w dt = 2Sat^{*1/2} \quad (29)$$

where t^* is the time at which the imbibition front arrives at the no flow boundary.^{45,46} Using eqs 28 and 29, the ratio of the cumulative recovery at time t to the ultimate cumulative recovery can be written as

$$\frac{Q}{Q_\infty} = \left(\frac{t}{t^*} \right)^{1/2} \quad (30)$$

To obtain the reference time t^* , for the case where the imbibition front hits the no flow boundary, it can be written that^{45,46}

$$x(S_{wi}, t^*) = L_c \quad (31)$$

from which using this equation and eq 26, t^* can be formulated as^{45,46}

$$t^* = \left(\frac{\phi L_c}{2AF'(S_{wi})} \right)^2 \quad (32)$$

Table 3. Summary of Different Cases of Common Scaling Practices and the Corresponding Scaling Equations

scaling case	y axis on scaling plot	corresponding x axis on scaling plot (i.e., scaling group)
normalizing experimental NWP recovery to final recovery	$\frac{Q}{Q_\infty}$	$t_{D,new} = \frac{2AF'(S_{wi})}{\phi L_c} t^{1/2}$
normalizing experimental NWP recovery to pore volume	$\frac{Q}{V_p}$	$t_{D,new} V_p = \frac{2A}{\phi L_c} t^{1/2}$
normalizing experimental NWP recovery to initial NWP volume in place	$\frac{Q}{V_i}$	$t_{D,new} V_i = \frac{2A}{\phi L_c(1 - S_{wi})} t^{1/2}$

Table 4. Summary of Different Cases of Common Scaling Practices and the Corresponding Darcy and Capillary Numbers

scaling case	Darcy number	capillary number
normalizing experimental NWP recovery to final recovery	$\frac{k}{\phi L_c^2}$	$\frac{\nu_w \mu_w}{\sigma} \int_{S_{wi}}^{S_{w,BC}} \frac{(S_{wi} - S_w) f(S_w) \frac{\mu_w k_{rw}}{\mu_{nw}} \frac{dS_w}{dS_w}}{F(S_w)} dS_w$
normalizing experimental NWP recovery to pore volume	$\frac{k}{\phi L_c^2}$	$\frac{\nu_w \mu_w}{\sigma} \int_{S_{wi}}^{S_{w,BC}} \frac{f(S_w) \frac{\mu_w k_{rw}}{\mu_{nw}} \frac{dS_w}{dS_w}}{F(S_w)} dS_w$
normalizing experimental NWP recovery to initial NWP volume in place	$\frac{k}{\phi L_c^2}$	$\frac{\nu_w \mu_w}{\sigma (1 - S_{wi})} \int_{S_{wi}}^{S_{w,BC}} \frac{f(S_w) \frac{\mu_w k_{rw}}{\mu_{nw}} \frac{dS_w}{dS_w}}{F(S_w)} dS_w$

Combining eqs 23, 30, and 32 yields

$$\frac{Q}{Q_\infty} = \frac{2AF'(S_{wi})}{\phi L_c} t^{1/2} = \frac{2A^2 F'(S_{wi})}{u_w \phi L_c} \quad (33)$$

Inserting eqs 24 and 27 in eq 33 and using the relationships between the average linear velocity and Darcy velocity, eq 8, and between the capillary pressure and Leverett dimensionless capillary pressure function, eq 14, then eq 33 can be written as

$$\frac{Q}{Q_\infty} = \frac{\sqrt{\frac{k}{\phi}}}{L_c} \frac{\sigma}{\nu_w \mu_w} \frac{\left(\int_{S_{wi}}^{S_{w,BC}} \frac{f(S_w) \frac{\mu_w k_{rw}}{\mu_{nw}} \frac{dS_w}{dS_w}}{F(S_w)} dS_w \right)^2}{\int_{S_{wi}}^{S_{w,BC}} \frac{(S_{wi} - S_w) f(S_w) \frac{\mu_w k_{rw}}{\mu_{nw}} \frac{dS_w}{dS_w}}{F(S_w)} dS_w} \quad (34)$$

The generalized Darcy number, Da, defined as the ratio of two characteristics lengths, pore and domain, can be written as

$$Da = \frac{k}{\phi L_c^2} \quad (35)$$

The generalized Capillary number, Ca, representing the relative effect of viscous forces versus interfacial tension can further be written as

$$Ca = \frac{\nu_w \mu_w \int_{S_{wi}}^{S_{w,BC}} \frac{(S_{wi} - S_w) f(S_w) \frac{\mu_w k_{rw}}{\mu_{nw}} \frac{dS_w}{dS_w}}{F(S_w)} dS_w}{\sigma \left(\int_{S_{wi}}^{S_{w,BC}} \frac{f(S_w) \frac{\mu_w k_{rw}}{\mu_{nw}} \frac{dS_w}{dS_w}}{F(S_w)} dS_w \right)^2} \quad (36)$$

Therefore, eq 34 can be rewritten as

$$\frac{Q}{Q_\infty} = \frac{Da^{1/2}}{Ca} \quad (37)$$

This equation shows that the recovery during COUCSI is controlled by the Darcy and the Capillary numbers. As a result, the solution obtained from one system is therefore applicable to other ones, because scaling the governing equations was performed in a consistent way obeying the general common scaling requirements. The dimensionless time can therefore be derived as the ratio between recoveries at time t to the ultimate recovery as

$$t_{D,new} = \frac{Q}{Q_\infty} = \frac{Da^{1/2}}{Ca} = \frac{2AF'(S_{wi})}{\phi L_c} t^{1/2} \quad (38)$$

The equation contains all relevant parameters related to the COUCSI process and therefore represents a consistent scaling equation, derived based on Rapoport's scaling requirement and by redefining the classical convention. In order to obtain stringent consistent diagrams, NWP recovery as fraction of

Table 5. Summary of Data for Experiments Performed by Bourbiaux and Kalaydjian^{52a}

expt.	S_{wi} (fraction)	L_c (m)	k (m ²)	ϕ (fraction)	μ_w (mPa s)	μ_{nw} (mPa s)	σ (N/m)	$F'(S_{wi})$ (-)	A ($\frac{m}{\sqrt{s}}$)
BK1	0.4	0.29	1.24×10^{-13}	0.233	1.2	1.5	0.035	5.2	1.14×10^{-05}
BK2	0.41	0.145	1.18×10^{-13}	0.233	1.2	1.5	0.035	4.85	9.66×10^{-06}

^aIn experiment BK1, the top end of the matrix was open to flow, whereas for BK2, both the bottom and top ends were allowed to fluid exchange. The porous media were SWW parallelepiped sandstone, and initial WP saturation was present.

Table 6. Summary of Data for Experiments Performed by Ma et al.^{16a}

expt.	S_{wi} (fraction)	L_c (m)	k (m ²)	ϕ (fraction)	μ_w (mPa s)	μ_{nw} (mPa s)	σ (N/m)	$F'(S_{wi})$ (-)	A ($\frac{m}{\sqrt{s}}$)
MZM1	0	0.01269	8.30×10^{-13}	0.229	0.9	4	0.047	1.79	5.21×10^{-05}
MZM2	0	0.01271	8.12×10^{-13}	0.228	0.9	10.6	0.049	1.8	2.83×10^{-05}
MZM3	0	0.01271	8.56×10^{-13}	0.225	0.9	37.8	0.051	1.64	2.73×10^{-05}

^aIn experiments, all faces of cores were open to flow. The porous media were SWW cylindrical Berea sandstone, and initial WP saturation was zero.

Table 7. Summary of Data for Experiments Performed by Zhou et al.^{53a}

expt.	S_{wi} (fraction)	L_c (m)	k (m ²)	ϕ (fraction)	μ_w (mPa s)	μ_{nw} (mPa s)	σ (N/m)	$F'(S_{wi})$ (-)	A ($\frac{m}{\sqrt{s}}$)
ZMM1	0.15	0.0126	3.55×10^{-13}	0.215	0.967	39.25	0.0242	3.53	1.39×10^{-06}
ZMM2	0.15	0.0126	3.65×10^{-13}	0.214	0.967	39.25	0.0242	4.07	7.37×10^{-07}
ZMM3	0.15	0.0126	3.00×10^{-13}	0.225	0.967	39.25	0.0242	4.63	1.88×10^{-07}

^aIn experiments, all faces of cores were open to flow. The porous media were MW cylindrical Berea sandstone, and initial WP saturation was present.

Table 8. Summary of Data for Experiments Performed by Fischer and Morrow^{20a}

expt.	S_{wi} (fraction)	L_c (m)	k (m ²)	ϕ (fraction)	μ_w (mPa s)	μ_{nw} (mPa s)	σ (N/m)	$F'(S_{wi})$ (-)	A ($\frac{m}{\sqrt{s}}$)
FM1	0	0.01238	6.51×10^{-14}	0.17	1.1	22	0.052	2.43	9.96×10^{-06}
FM2	0	0.01242	6.54×10^{-14}	0.17	4.4	22	0.041	1.96	8.01×10^{-06}
FM3	0	0.0124	6.88×10^{-14}	0.168	8.7	22	0.037	1.91	6.54×10^{-06}
FM4	0	0.01239	6.97×10^{-14}	0.171	15.2	22	0.036	2.24	5.19×10^{-06}
FM5	0	0.01241	6.55×10^{-14}	0.17	22	22	0.035	2.16	4.40×10^{-06}
FM6	0	0.01238	6.61×10^{-14}	0.169	39.6	22	0.033	2.27	4.62×10^{-06}
FM7	0	0.01239	6.80×10^{-14}	0.169	96.6	22	0.033	1.95	3.22×10^{-06}
FM8	0	0.01236	6.97×10^{-14}	0.16	228.4	22	0.031	1.79	1.66×10^{-06}
FM9	0	0.01219	6.78×10^{-14}	0.174	1646.6	22	0.029	1.15	9.23×10^{-07}

^aIn experiments, all faces of cores were open to flow. The porous media were SWW cylindrical Berea sandstone, and initial WP saturation was zero.

Table 9. Summary of Data for Experiments Performed by Fischer et al.^{21a}

expt.	S_{wi} (fraction)	L_c (m)	k (m ²)	ϕ (fraction)	μ_w (mPa s)	μ_{nw} (mPa s)	σ (N/m)	$F'(S_{wi})$ (-)	A ($\frac{m}{\sqrt{s}}$)
FWM1	0	0.0124	6.23×10^{-14}	0.169	4.4	3.9	0.0398	1.84	7.39×10^{-06}
FWM2	0	0.0124	6.27×10^{-14}	0.168	99.8	3.9	0.0312	2.14	2.92×10^{-06}
FWM3	0	0.0123	1.12×10^{-13}	0.186	1	63.3	0.0513	2.08	1.37×10^{-05}
FWM4	0	0.0123	1.48×10^{-13}	0.192	4.1	63.3	0.0417	1.97	9.60×10^{-06}
FWM5	0	0.0123	1.37×10^{-13}	0.191	27.8	63.3	0.0348	2.04	4.60×10^{-06}
FWM6	0	0.0124	1.44×10^{-13}	0.191	97.7	63.3	0.0321	1.76	3.36×10^{-06}
FWM7	0	0.0134	1.47×10^{-13}	0.193	1	3.9	0.0505	1.78	2.10×10^{-05}
FWM8	0	0.0134	1.49×10^{-13}	0.193	4.1	3.9	0.0412	1.45	1.43×10^{-05}
FWM9	0	0.0134	1.45×10^{-13}	0.191	97.7	3.9	0.0313	1.55	3.31×10^{-06}
FWM10	0	0.0134	1.47×10^{-13}	0.19	494.6	3.9	0.0289	1.41	1.80×10^{-06}
FWM11	0	0.0134	1.06×10^{-13}	0.186	1	63.3	0.0513	1.73	1.16×10^{-05}
FWM12	0	0.0134	1.46×10^{-13}	0.187	4.1	63.3	0.0417	2.09	9.00×10^{-06}
FWM13	0	0.0134	1.38×10^{-13}	0.191	27.8	63.3	0.0348	1.5	4.27×10^{-06}
FWM14	0	0.0134	1.28×10^{-13}	0.188	97.7	63.3	0.0321	1.72	2.94×10^{-06}
FWM15	0	0.0134	1.54×10^{-13}	0.192	494.6	63.3	0.0298	1.75	1.47×10^{-06}
FWM16	0	0.0134	1.51×10^{-13}	0.198	1	173.1	0.0528	1.76	1.05×10^{-05}
FWM17	0	0.0134	1.39×10^{-13}	0.194	4.9	173.1	0.0431	1.59	8.15×10^{-06}

^aThe porous media were SWW cylindrical Berea sandstone, and initial WP saturation was zero. The tests FWM1 to FWM6 are for the all faces open boundary condition, whereas tests FWM7 to FWM17 are for the two ends closed configuration.

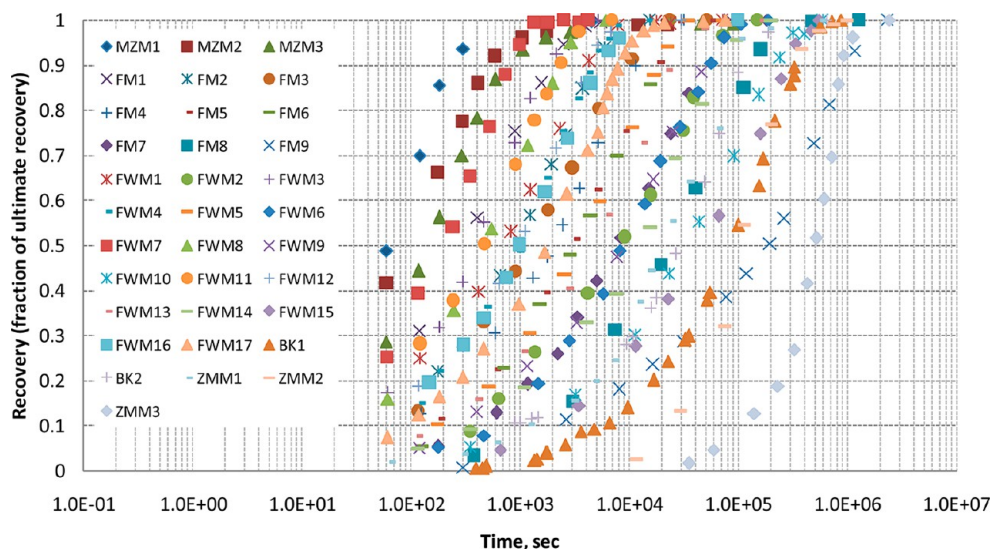


Figure 1. Recovery in terms of ultimate recovery versus time for experiments collected from the literature. Experimental SWW data from Bourbiaux and Kalaydjian,⁵² Ma et al.,¹⁶ Fischer and Morrow,²⁰ and Fischer et al.²¹ and also MW data from Zhou et al.⁵³ are represented, respectively, as “BK,” “MZM,” “FM,” “FWM,” and “ZMM.”

recoverable NWP should be plotted versus $t_{D,new}$. It should be noticed that it is crucial to use exactly the expression Q/Q_∞ on the vertical axis and $t_{D,new}$ on the horizontal axis. Normalizing

NWP recovery to pore volume, PV, or initial NWP in place will, for example, shift the relative position of the observed data along the new dimensionless time axis.

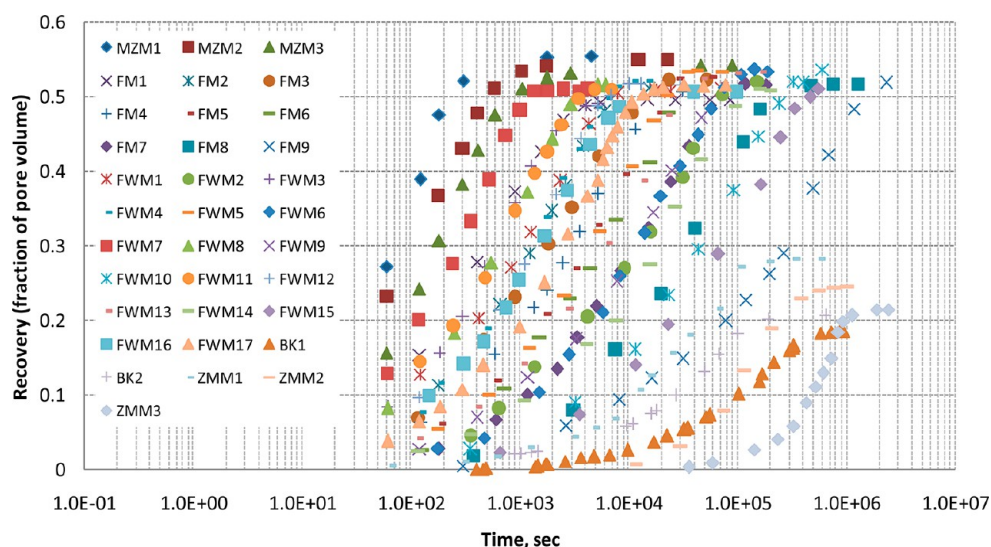


Figure 2. Recovery in terms of pore volume versus time for experiments collected from the literature. Experimental SWW data from Bourbiaux and Kalaydjian,⁵² Ma et al.,¹⁶ Fischer and Morrow,²⁰ and Fischer et al.²¹ and also MW data from Zhou et al.⁵³ are represented, respectively, as “BK,” “MZM,” “FM,” “FWM,” and “ZMM.”

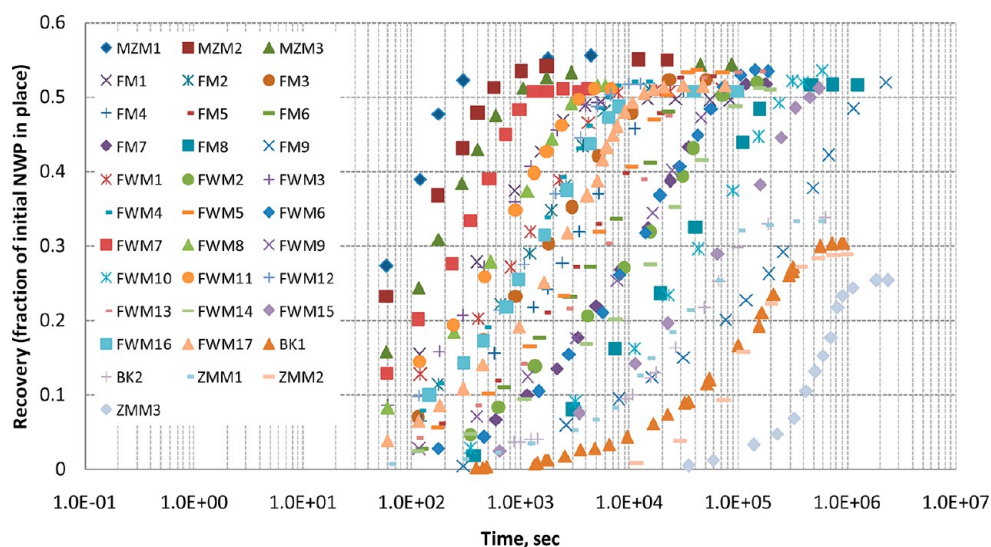


Figure 3. Recovery in terms of initial NWP in place versus time for experiments collected from the literature. Experimental SWW data from Bourbiaux and Kalaydjian,⁵² Ma et al.,¹⁶ Fischer and Morrow,²⁰ and Fischer et al.²¹ and also MW data from Zhou et al.⁵³ are represented, respectively, as “BK,” “MZM,” “FM,” “FWM,” and “ZMM.”

The main advantage of using the consistency outlined through eq 38 is that all scaling equations then can directly be scaled up to any dimension or change in system parameters in a consistent and stringent way because all requirements given by Rapoport's analysis are fulfilled. If normalizing experimental NWP recovery to pore volume V_p is preferred, then dimensionless time shown in eq 38 does not hold anymore, and for this case, the corresponding dimensionless time equation $t_{D,newV_p}$ should be defined accordingly. Therefore, in this case, in order to obtain stringent consistent diagrams, NWP recovery as fraction of pore volume should be plotted versus $t_{D,newV_p}$. It should be noticed that it is crucial to use exactly the expression Q/V_p on the vertical axis and $t_{D,newV_p}$ on the horizontal axis. If normalizing experimental NWP recovery to initial NWP in place V_i is preferred, then for this case the corresponding dimensionless time equation $t_{D,newV_i}$ should be defined accordingly. In this case, in order to obtain stringent consistent diagrams, NWP recovery as a fraction of V_i should be plotted versus $t_{D,newV_i}$.

It should be noticed that it is crucial to use exactly the expression Q/V_i on the vertical axis and $t_{D,newV_i}$ on the horizontal axis. We should note that for the two latter cases, the corresponding capillary numbers can be defined. Different cases of scaling and corresponding scaling equations (or dimensionless times) are listed in Table 3. Furthermore, Table 4 contains a summary of different cases of scaling practices and corresponding Darcy and capillary numbers. The new scaling equations resolve all limitations of scaling groups published during past decades. Furthermore, to account for directional permeability within the matrix block, the permeability k in the new scaling equations can be replaced by the new definition of the characteristic permeability k_c defined in eq 1.

Considering the above formulations, it can be shown that

$$\left(\frac{Q}{V_p}\right)^2 = \left(\frac{2A}{\phi L_c}\right)^2 t \quad (39)$$

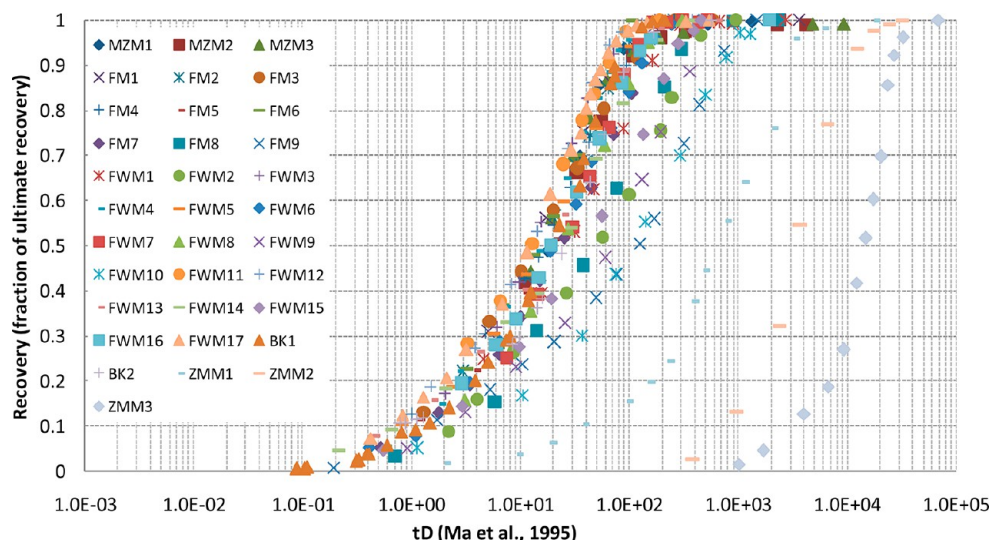


Figure 4. Experimental recovery in terms of ultimate recovery versus scaling equation of Ma et al.¹⁶ This scaling equation scales data of SWW systems well only for the cases where WP and NWP viscosities are close to each other. However, as the viscosity of one of these phases becomes much greater than the other one, the spread in the data increases. This scaling equation also does not account for variations in wettability, and the curves for MW systems systematically lie to the right of the SWW curves.

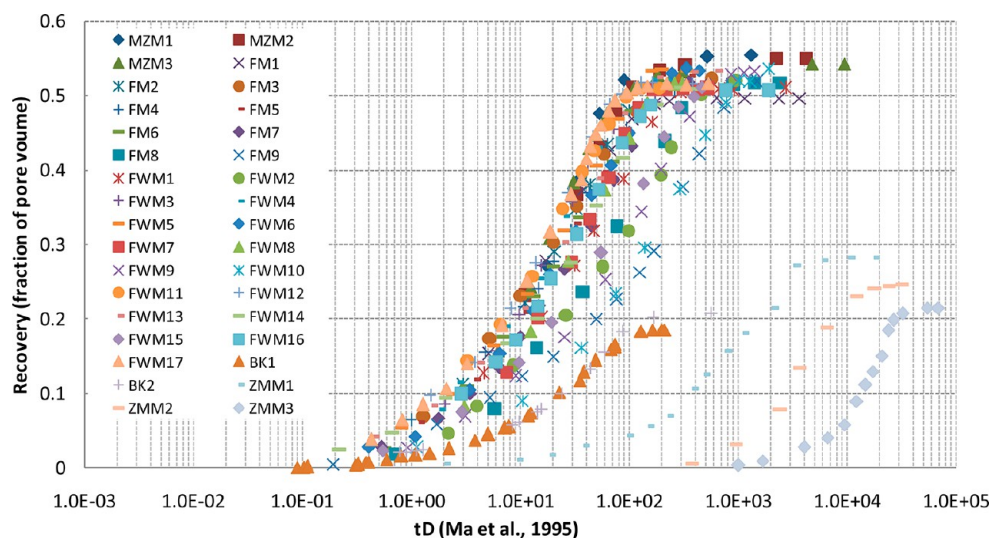


Figure 5. Experimental recovery in terms of pore volume versus scaling equation of Ma et al.¹⁶ This scaling equation scales data of SWW systems well only for the cases where WP and NWP viscosities are close to each other. However, as the viscosity of one of these phases becomes much greater than the other one, the spread in the data increases. This scaling equation also does not account for variations in wettability, and the curves for MW systems systematically lie to the right of the SWW curves.

Schmid and Geiger^{45,46} used the right-hand side of this equation and defined their scaling equation $t_{D,SG}$ as

$$t_{D,SG} = \left(\frac{2A}{\phi L_c} \right)^2 t \quad (40)$$

Investigation of eq 39 shows that the $t_{D,SG}$ has been defined by squaring the ratio of the recovery to the pore volume obeying the classical convention. This implies that when using this scaling equation it is crucial to put exactly the $(Q/V_p)^2$ on the vertical axis and $t_{D,SG}$ on the horizontal axis to get a correct scaling result. However, such a form of scaling (i.e., putting the squared recovery on the vertical axis) is not common in scaling studies. Using their scaling equation in common scaling practices may result in nontrivial scatter in scaling plots

(see Figure 4 in ref 45 and Figures 5b and 8b,c in ref 46), as will be shown later using experimental data.

As discussed before, in practice spontaneous imbibition can occur under a variety of wetting conditions including SWW, WWW, MW, and FW, each with different extents.³³ For SWW systems, the water saturation reached at the end of spontaneous imbibition ($S_{wf,SI}$) can be assumed to be the same as that reached at the end of further forced displacement ($S_{wf,FD}$). For such systems, the capillary pressure is positive over the whole saturation range from S_{wi} to $S_{wf,SI} = S_{wf,FD}$. In this range of saturation, since $(dP_c)/(dS_w)$ is negative, therefore according to eq 3 $D(S_w)$ is positive. Under this circumstance, eq 2 predicts that spontaneous imbibition continues to $S_{wf,SI} = S_{wf,FD}$ as long as the $S_{w,BC}$ is greater than the S_{wi} . This behavior is reasonable, resulting in validity of the governing equation eq 2 in simulating the process in SWW systems.

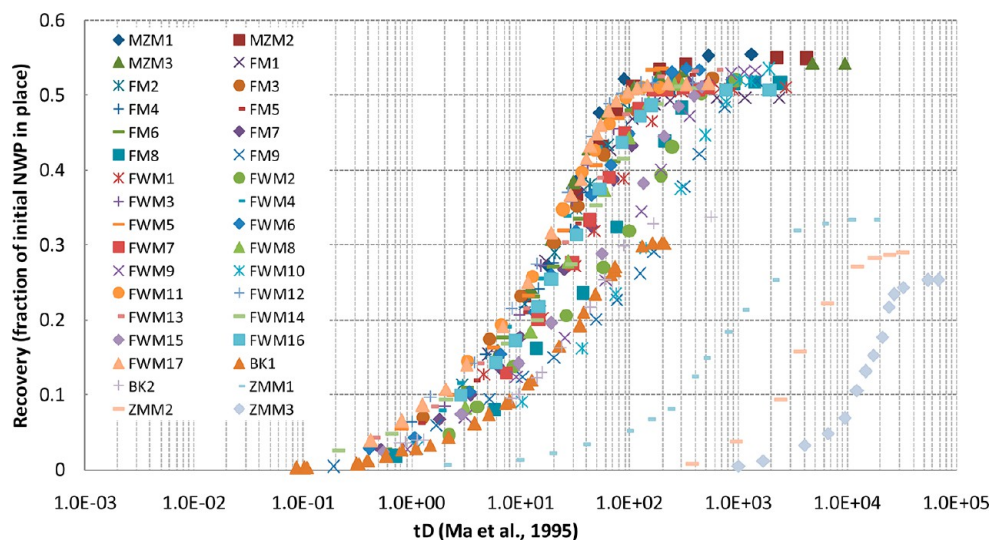


Figure 6. Experimental recovery in terms of initial NWP in place versus scaling equation of Ma et al.¹⁶ This scaling equation scales data of SWW systems well only for the cases where WP and NWP viscosities are close to each other. However, as the viscosity of one of these phases becomes much greater than the other one, the spread in the data increases. This scaling equation also does not account for variations in wettability, and the curves for MW systems systematically lie to the right of the SWW curves.

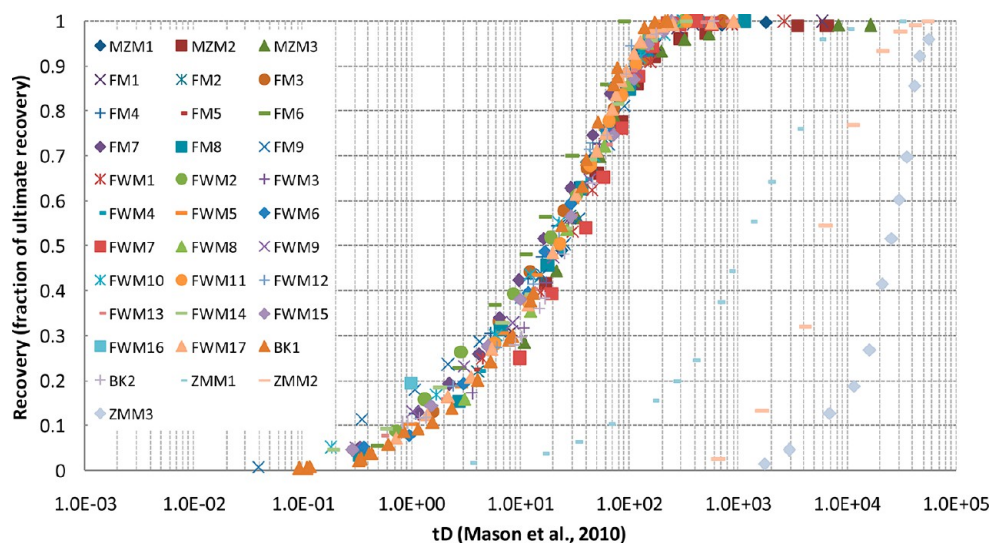


Figure 7. Recovery in terms of ultimate recovery versus scaling equation of Mason et al.²³ This scaling equation scales data of SWW systems very well even for the cases which WP and NWP viscosities are not close to each other. This scaling equation, however, does not account for variations in wettability, and the curves for MW systems systematically lie to the right of the SWW curves.

However, in practice, for WWW, MW, and FW systems, $S_{wf,SI}$ is less than $S_{wf,FD}$. In these systems, capillary pressure is positive from S_{wi} to $S_{wf,SI}$ and negative from $S_{wf,SI}$ to $S_{wf,FD}$, and $(dP_c)/(dS_w)$ is negative over the whole saturation range, including the first range from S_{wi} to $S_{wf,SI}$ and the second range from $S_{wf,SI}$ to $S_{wf,FD}$. For such cases, according to eq 3 the $D(S_w)$ is positive over the both ranges, and eq 2 wrongly predicts that spontaneous imbibition continues until $S_{wf,FD}$ as long as the $S_{w,BC}$ is greater than the S_{wi} mainly because the problem is not a pressure boundary condition. This behavior was noticed and discussed in detail by Schmid and Geiger.⁴⁶ To make the prediction of analytical solution consistent with the real physics of the problem, Schmid and Geiger⁴⁶ proposed two methods. In the first method, it was assumed that $S_{w,BC} = S_{wf,FD}$ and $P_c = 0$ after $S_{wf,SI}$ resulting in $(dP_c)/(dS_w) = 0$ from $S_{wf,SI}$ to $S_{wf,FD}$. Using this method, $D(S_w)$ would be zero after $S_{wf,SI}$ and therefore the analytical solution will predict no further

spontaneous imbibition after $S_{wf,SI}$. In the second method, it was assumed that $S_{w,BC} = S_{wf,SI}$. Clearly for such a case, the capillary pressure and relative permeability data up to $S_{wf,SI}$ are used in computations. They recommended the second method because it is based on all the information present in a spontaneous imbibition system and therefore has a sound physical justification. Using such a technique, Schmid and Geiger⁴⁶ successfully extended their previous scaling equation (Schmid and Geiger⁴⁵), which was first derived for SWW conditions, to other wettability conditions under which spontaneous imbibition may occur.

At this step, as promised before to derive eq 8, inserting eq 32 in eq 29 gives

$$Q_\infty = \frac{S\phi L_c}{F'(S_{wi})} \quad (41)$$

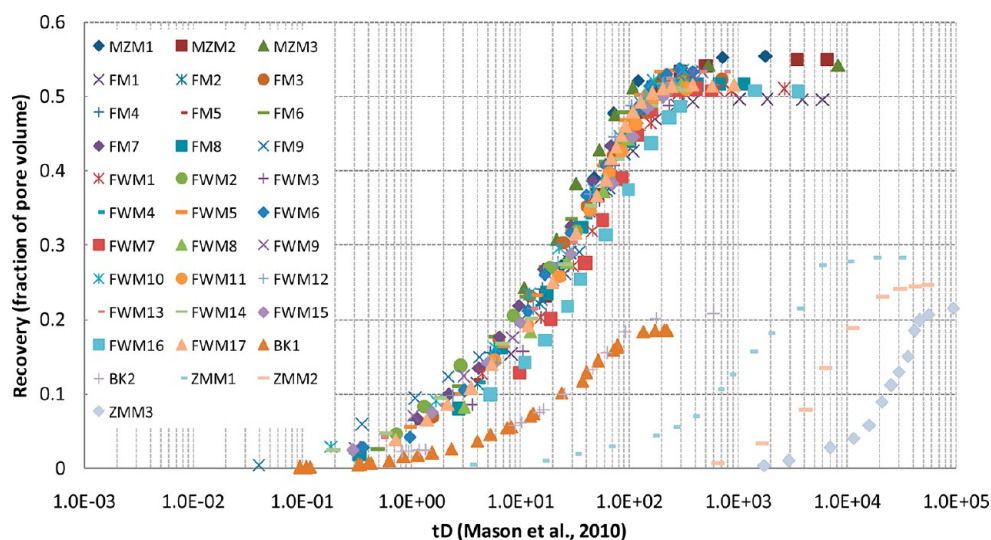


Figure 8. Recovery in terms of pore volume versus scaling equation of Mason et al.²³ This scaling equation scales data of SWW systems very well even for the cases which WP and NWP viscosities are not close to each other. This scaling equation, however, does not account for variations in wettability, and the curves for MW systems systematically lie to the right of the SWW curves.

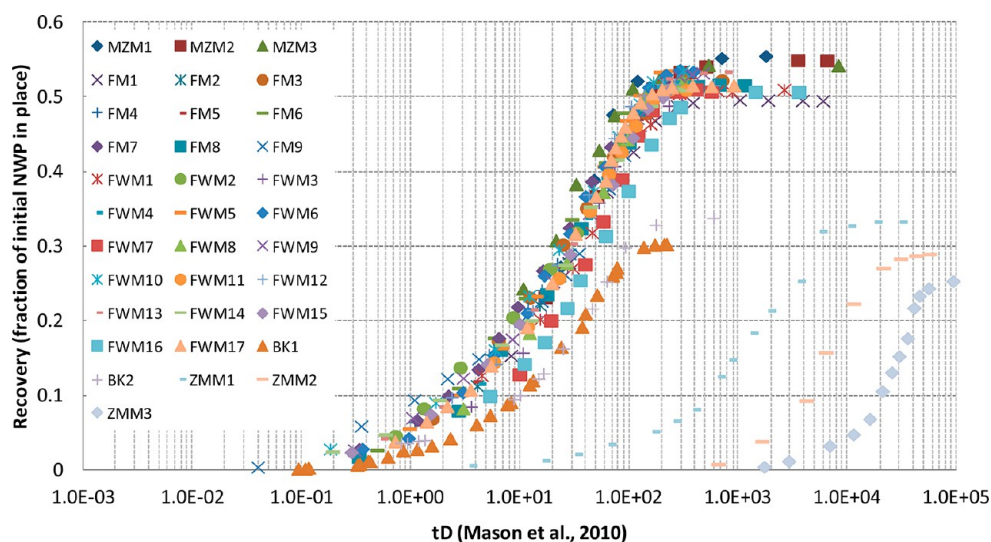


Figure 9. Recovery in terms of initial NWP in place versus the scaling equation of Mason et al.²³ This scaling equation scales data of SWW systems very well even for the cases in which WP and NWP viscosities are not close to each other. This scaling equation, however, does not account for variations in wettability, and the curves for MW systems systematically lie to the right of the SWW curves.

Dividing both sides of the resulting equation by pore volume gives

$$\frac{Q_{\infty}}{V_p} = \frac{1}{F'(S_{wi})} \quad (42)$$

Equation 8 then can be automatically resulted from the above equation since the fraction of pore volume that is ultimately recovered is $1(F'(S_{wi}))$.

Furthermore, to derive eq 17, using eq 26, we can write

$$t^{1/2} = \frac{\phi x(S_w, t)}{2AF'(S_w)} \quad (43)$$

Inserting eq 43 into eq 33 then gives eq 17.

4. VALIDATION OF THE NEW SCALING EQUATIONS

We collected data sets of COUCSI experiments covering a relatively wide range in the major parameters affecting the process like boundary conditions, WP and NWP viscosities,

absolute permeability, initial WP saturation, and wettability. It was attempted to use the reference works providing the maximum required data. For this purpose, the published experimental data by Bourbiaux and Kalaydjian,⁵² Ma et al.,¹⁶ Zhou et al.,⁵³ Fischer and Morrow,²⁰ and Fischer et al.²¹ were used (see, respectively Tables 5, 6, 7, 8, and 9). All the data are from cylindrical Berea sandstone samples except those of Bourbiaux and Kalaydjian,⁵² who performed the tests on parallelepiped sandstone (from the Vosges region, France) samples. Data from Bourbiaux and Kalaydjian,⁵² Ma et al.,¹⁶ Zhou et al.,⁵³ Fischer and Morrow,²⁰ and Fischer et al.²¹ are represented, respectively, as “BK,” “MZM,” “ZMM,” “FM,” and “FWM.” All experiments were performed on SWW systems except those of Zhou et al.,⁵³ which reported imbibition tests on MW systems (their core numbers 11, 12, and 13 each, respectively, corresponding to aging times of 4, 48, and 72 h).

In the experiments performed by Bourbiaux and Kalaydjian⁵² for the case of BK1, only one end of the matrix was open to

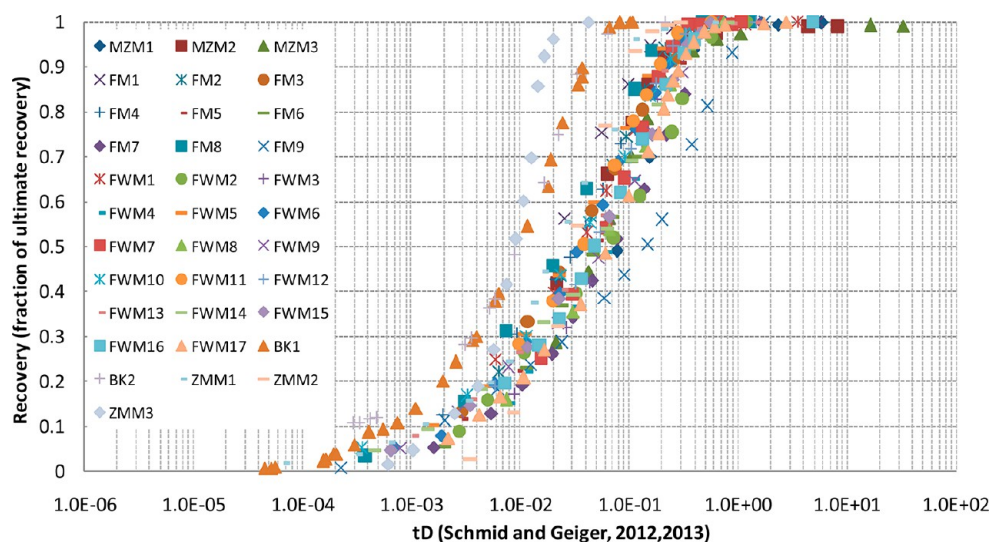


Figure 10. Recovery in terms of ultimate recovery versus the scaling equation of Schmid and Geiger.^{45,46} The results show still a scatter in the scaled imbibition curves. Our study shows that the reason for such scatter is mainly because their scaling equation is not according to common scaling practices.

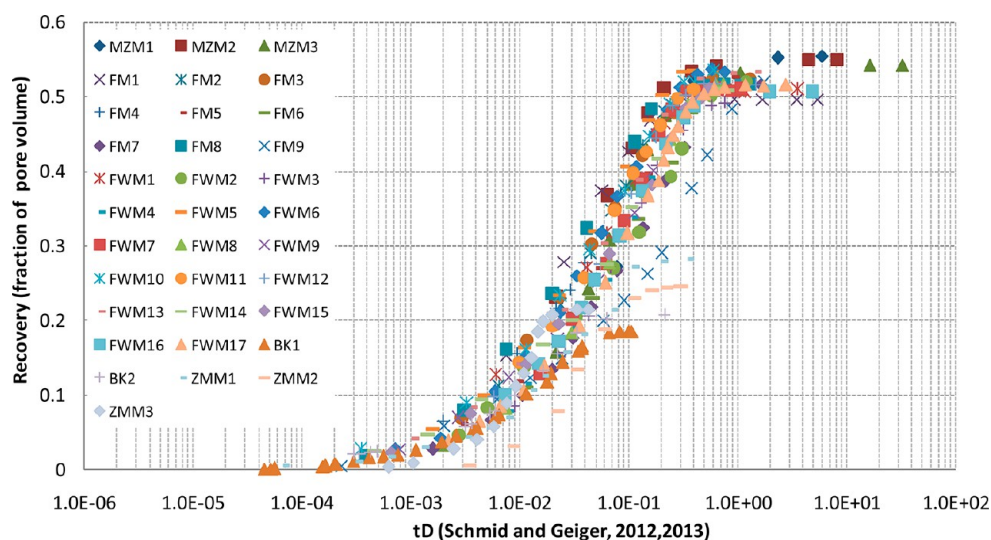


Figure 11. Recovery in terms of pore volume versus scaling equation of Schmid and Geiger.^{45,46} The results show still a scatter in the scaled imbibition curves. Our study shows that the reason for such scatter is mainly because their scaling equation is not according to common scaling practices.

flow (i.e., linear flow), whereas for BK2 both ends were open to fluid exchange (i.e., linear flow). Furthermore, in experiments conducted by Ma et al.,¹⁶ Zhou et al.,⁵³ and Fischer and Morrow,²⁰ all faces of the matrix were open to flow (i.e., linear + radial flow). For experiments run by Fischer et al.,²¹ the tests FWM1 to FWM6 are for the all faces open boundary condition (i.e., linear + radial flow), whereas tests FWM7 to FWM17 are for the two ends closed configuration (i.e., radial flow). The characteristic length values are obtained using the definition proposed by Ma et al.¹⁶ The recovery curves versus time of all data are shown in Figures 1, 2, and 3. In the experiments which we use for validation, the permeability only in one direction was reported. Therefore, we assume the same permeability in all directions making the characteristic permeability the same as the single-direction reported permeability.

The ability of the new scaling equations to scale data is compared to other well-established scaling equations. The well-known and widely used scaling equations proposed by Ma et al.,¹⁶ Mason et al.,²³ and Schmid and Geiger^{45,46} were used for comparison purposes. These scaling equations, as discussed,

are based on the classical convention. To utilize the scaling equations of Ma et al.¹⁶ and Mason et al.,²³ the only data needed are routine core and fluid properties, as listed in Tables 5–9 for each specific experiment. However, to use the scaling equation of Schmid and Geiger^{45,46} and the consistent scaling equations presented in this study, capillary pressure and relative permeability data are needed, as well. Comprehensive studies reporting COUCSI recovery, capillary pressure, and relative permeability data are extremely rare in the literature. For experiments from Bourbiaux and Kalaydjian,⁵² however, the capillary pressure and history matched relative permeability data were reported. Schmid and Geiger⁴⁵ therefore assumed that, for the case of SWW Berea sandstone systems, the reported relative permeability and capillary pressure sets obtained from pore network modeling reported for a certain rock type (Valvatne and Blunt⁵⁴) were representative for a given material, and they used these data when testing their scaling equation. For the case of MW experiments done by Zhou et al.,⁵³ Schmid and Geiger⁴⁶ used the capillary pressure and relative permeability

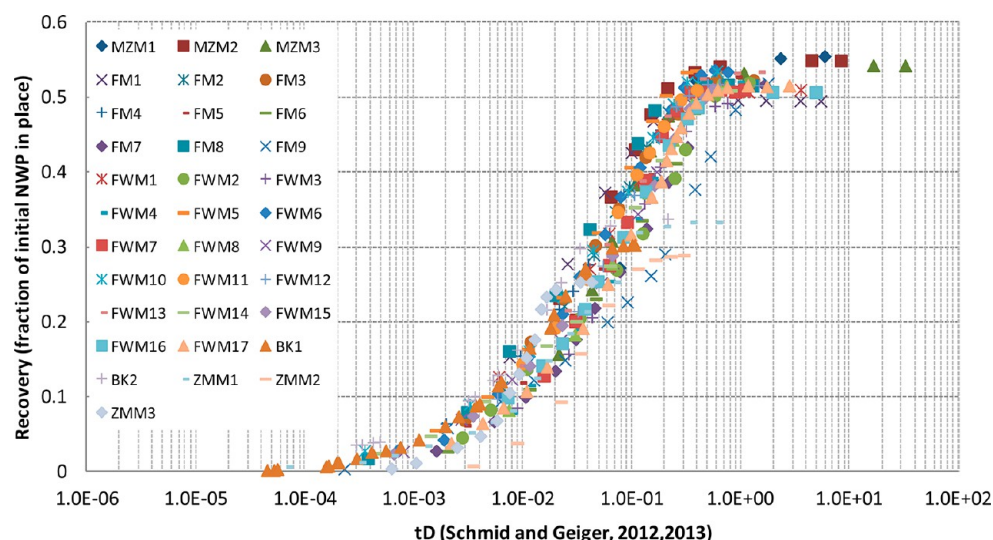


Figure 12. Recovery in terms of initial NWP in place versus the scaling equation of Schmid and Geiger.^{45,46} The results show still a scatter in the scaled imbibition curves. Our study shows that the reason for such scatter is mainly because their scaling equation is not according to common scaling practices.

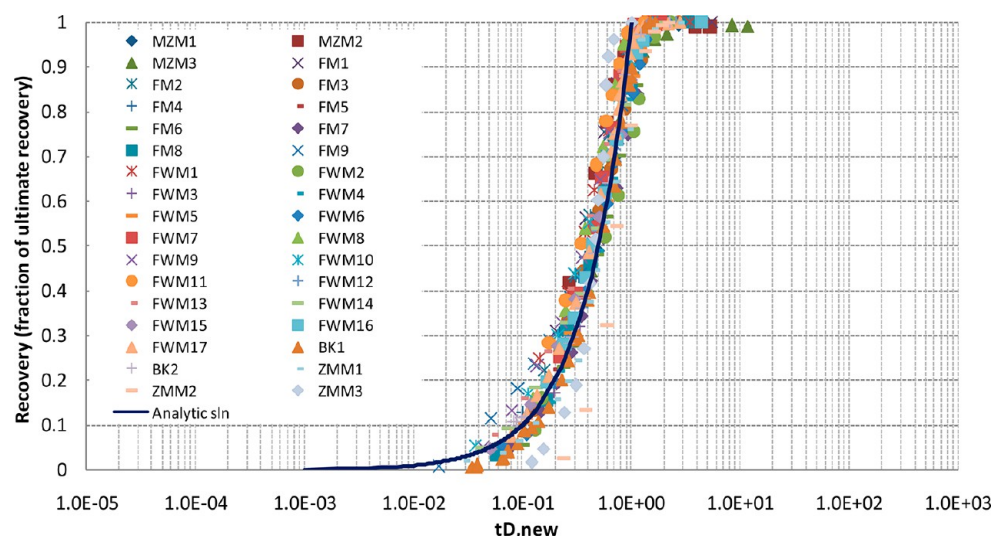


Figure 13. Recovery in terms of ultimate recovery versus the corresponding new scaling equation. The scaling result indicates a significant improvement compared to the previous scaling equations. The new scaling equation collapses all the recovery curves of SWW and MW systems perfectly into a single universal curve including large variations in viscosity ratio.

data generated for these experiments using pore network modeling (Behbahani and Blunt²⁷). We have followed the same approach.

Since the scaling equation of Ma et al.,¹⁶ and also Mason et al.,²³ was derived based on application of general principles of dimensional analysis (Rapoport¹²), rather than by a mathematical treatment, establishing a true exact relationship between the vertical and horizontal axes in scaling plots is not possible. Thus in scaling plots, the vertical axis may be recovery normalized by either the final recovery, pore volume, or initial NWP in place. Figures 4, 5, and 6 show the ability of the scaling equation of Ma et al.¹⁶ to scale the data when the recovery normalized by either the ultimate recovery (Figure 4), pore volume (Figure 5), or initial NWP in place (Figure 6) is plotted versus their scaling equation. Figures 4, 5, and 6 show that the scaling equation of Ma et al.¹⁶ scales data of SWW systems well only for the cases where WP and NWP viscosities are close to each other. However, as the viscosity of one of these phases becomes much greater than the other one, the spread in the

data increases. The figures also show that this scaling equation does not account for variations in wettability because the curves for MW systems systematically lie to the right of the SWW curves, meaning that a longer dimensionless time is needed for the MW cases than for the SWW cases to obtain the same normalized recovery.

Figures 7, 8, and 9 show the ability of the scaling equation of Mason et al.²³ to scale the data when the recovery normalized by either the ultimate recovery (Figure 7), pore volume (Figure 8), or initial NWP in place (Figure 9) is plotted versus their scaling equation. Figures 7, 8, and 9 show that the scaling result is perfect even for large variations in viscosity ratio. However, like the scaling equation of Ma et al.,¹⁶ poor scaling results are obtained from the COUCSI results generated using MW systems. Two distinct groups of curves are identified for this scaling equation based on the system wettability, SWW, or MW, where the MW curves lie all systematically to the right of the SWW curves.

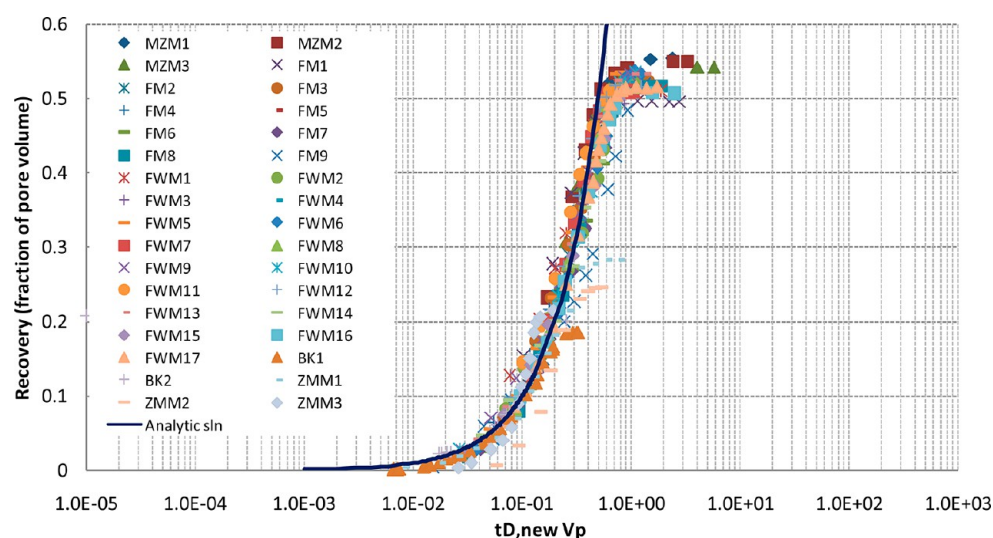


Figure 14. Recovery in terms of pore volume versus the corresponding new scaling equation. The scaling result indicates a significant improvement compared to the previous scaling equations. The new scaling equation collapses all the recovery curves of SWW and MW systems perfectly into a single universal curve including large variations in viscosity ratio.

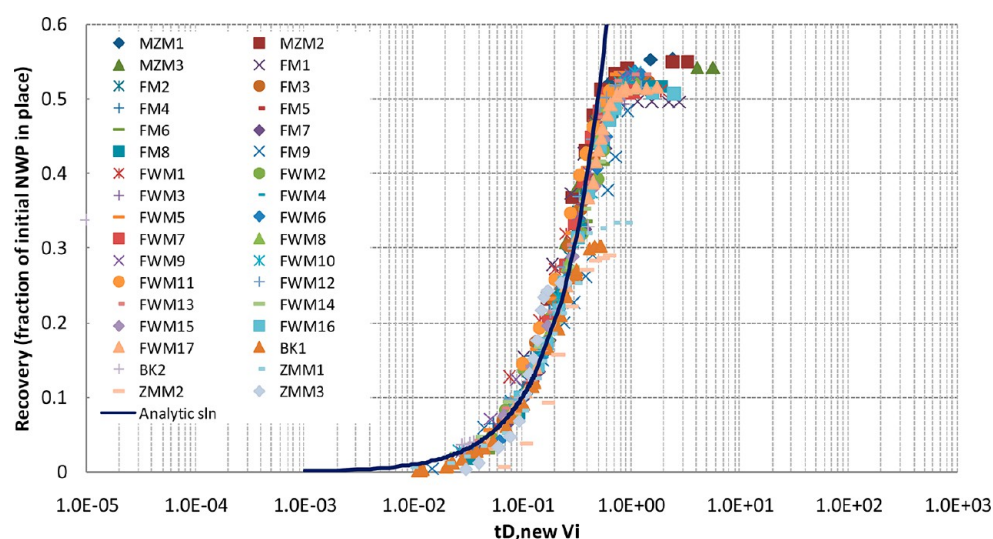


Figure 15. Recovery in terms of initial NWP in place versus the corresponding new scaling equation. The scaling result indicates a significant improvement compared to the previous scaling equations. The new scaling equation collapses all the recovery curves of SWW and MW systems perfectly into a single universal curve including large variations in viscosity ratio.

As discussed before, to use the scaling equation of Schmid and Geiger,^{45,46} the vertical axis in scaling plots should be the squared ratio of recovery to pore volume (which is of course not common and not shown here). Thus, when using their scaling equation, putting the recovery normalized by either final recovery, pore volume, or initial NWP in place on the vertical axis may cause poor scaling results. This behavior is shown in Figures 10, 11, and 12 for each of these situations.

Figures 13, 14, and 15 show the ability of the consistent scaling equations presented in this study to scale the data when the recovery normalized by either the ultimate recovery (Figure 13), pore volume (Figure 14), or initial NWP in place (Figure 15) is plotted versus the corresponding scaling equation (see Table 3). The scaling results indicate a significant improvement compared to the previous scaling equations. These scaling equations collapse all the recovery curves of SWW and MW systems into a single universal curve including large variations in viscosity ratio. We should note that for comparison between the scaling abilities of

different scaling equations, Figures 1–15 do have the same number of cycles, eight numbers, on their horizontal axes.

In Figures 13, 14, and 15, the curve given by the analytical solution is also included. The data in these figures do have less scatter around the analytical solution curve. We believe that even the lesser scatter can be observed if better predictions for the capillary-hydraulic properties are available.

5. CONCLUSIONS

Regarding the main subject of this work, which was to show that during development of any scaling equation its consistency with practice should be considered, the main conclusions drawn can be listed as follows:

The classical convention in which it is required to define the scaling equations by relating the squared recovery to squared pore volume is blind and does not apply to common scaling practices of oil/gas recovery by spontaneous imbibition.

For common scaling practices, depending on situation, as a criterion, scaling equations should correspond to equal normalized cumulative recoveries between model and prototype.

By extending the latest scaling work of Schmid and Geiger^{45,46} and by considering common scaling practices, consistent scaling equations can be found using the known analytical solution for an infinite acting period of COUCSI.^{43,44} These scaling equations incorporate the effect of all influencing parameters on COUCSI including different wettability states and high contrast in viscosities.

The consistent scaling equations can be expressed in terms of two well-known dimensionless numbers, $Da^{1/2}/Ca$ (Da , Darcy number; Ca , capillary number).

In applying the scaling equations for scaling purposes, one should use appropriate terms on the vertical and horizontal axes.

The effect of directional permeability should be incorporated into scaling equations.

AUTHOR INFORMATION

Corresponding Author

*Tel.: +982166166425. Fax: +982166022853. E-mail: Masihi@Sharif.edu.

Notes

The authors declare no competing financial interest.

ACKNOWLEDGMENTS

The authors appreciate very much the valuable comments from Dr. Dag Chun Standnes of Statoil. We also thank the Research and Technology Department of NISOC/NIOC.

REFERENCES

- (1) Warren, J. E.; Root, P. J. *SPE J.* **1963**, Sept., 245–255.
- (2) Cai, J.; Yu, B.; Zou, M.; Luo, L. *Energy Fuels* **2010**, *24*, 1860–1867, DOI: 10.1021/ef901413p.
- (3) Cai, J.; Yu, B. *Transp. Porous Media* **2011**, *89*, 251–263, DOI: 10.1007/s11242-011-9767-0.
- (4) Cai, J.; Hu, X.; Standnes, D. C.; You, L. *Colloids Surf., A* **2012**, *414*, 228–233, DOI: 10.1016/j.colsurfa.2012.08.047.
- (5) Ma, S.; Morrow, N. R.; Zhou, X.; Zhang, X. *J. Can. Pet. Technol.* **1999**, *38* (13), 1–8.
- (6) Dehghanpour, H.; Zubair, H. A.; Chhabra, A.; Ullah, A. *Energy Fuels* **2012**, *26*, 5750–5758.
- (7) Dehghanpour, H.; Lan, Q.; Saeed, Y.; Fei, H.; Qi, Z. *Energy Fuels* **2013**, *27* (6), 3039–3049, DOI: 10.1021/ef4002814.
- (8) Mirzaei-Paibaman, A.; Masihi, M.; Moghadasi, J. *SPE paper 129637, SPE Deep Gas Conference and Exhibition*, January, 24–26, 2010, Manama, Bahrain. DOI: 10.2118/129637-MS.
- (9) Mirzaei-Paibaman, A.; Dalvand, K.; Oraki, I.; Masihi, M.; Moghadasi, J. *Energy Sources, Part A* **2012**, *34*, 1541–1549, DOI: 10.1080/15567036.2010.489102.
- (10) Mirzaei-Paibaman, A.; Masihi, M.; Moghadasi, J. *Pet. Sci. Technol.* **2011**, *29*, 1–10, DOI: 10.1080/10916460903551073.
- (11) Li, K.; Horne, R. N. *Transp. Porous Media* **2009**, *83*, 699–709.
- (12) Rapoport, L. A. *Trans. AIME* **1955**, *204*, 143–150.
- (13) Mattax, C. C.; Kyte, J. R. *SPE J.* **1962**, *2* (2), 177–184.
- (14) Kazemi, H.; Merrill, L. S.; Porterfield, K. L.; Zeman, P. R. *SPE J.* **1976**, *16*, 317–326.
- (15) Kazemi, H.; Gilman, J. R.; Elsharkawy, A. M. *SPE Res. Eng.* **1992**, *7* (2), 219–227.
- (16) Ma, S.; Zhang, X.; Morrow, N. R. *Influence of Fluid Viscosity on Mass Transfer between Rock Matrix and Fractures*; Annual Technical Meeting, Jun 7–9, 1955, Calgary, Alberta; Petroleum Society of Canada: Calgary, Canada, 1955. DOI: 10.2118/95-94.
- (17) Zhang, X.; Morrow, N.; Ma, S. *SPE Res. Eng.* **1996**, *11* (4), 280–285.
- (18) Standnes, D. C. *Energy Fuels* **2004**, *18*, 271–282.
- (19) Yildiz, H. O.; Gokmen, M.; Cesur, Y. *J. Pet. Sci. Eng.* **2006**, *53*, 158–170.
- (20) Fischer, H.; Morrow, N. R. *J. Pet. Sci. Eng.* **2006**, *52* (1–4), 35–53.
- (21) Fischer, H.; Wo, S.; Morrow, N. R. *SPE Res. Eval. Eng.* **2008**, June, 577–589.
- (22) Mason, G.; Fischer, H.; Morrow, N. R.; Ruth, D. W.; Wo, S. *J. Pet. Sci. Eng.* **2009**, *66*, 83–97.
- (23) Mason, G.; Fischer, H.; Morrow, N. R.; Ruth, D. W. *J. Pet. Sci. Eng.* **2010**, *72*, 195–205.
- (24) Mason, G.; Fischer, H.; Morrow, N. R.; Ruth, D. W. *Transp. Porous Media* **2009**, *78*, 199–216, DOI: 10.1007/s11242-008-9296-7.
- (25) Heinemann, Z. E.; Mittermeir, G. M. *Transp. Porous Media* **2012**, *91*, 123–132, DOI: 10.1007/s11242-011-9836-4.
- (26) Gupta, A.; Civan, F. *SPE Paper 28929; SPE 69th Annual Technical Conference and Exhibition*, New Orleans, LA, U.S.A., Sept. 25–28, 1994.
- (27) Behbahani, H. S.; Blunt, M. J. *SPE J.* **2005**, *10* (4), 466–474.
- (28) Iffly, R.; Rousselet, D. C.; Vermeulen, J. L. *SPE Paper no. 4102; Proceedings of the 47th SPE Annual Fall Meeting of AIME*, San Antonio, Texas, October 8–11, 1972.
- (29) Cuiec, L.; Bourbiaux, B. J.; Kalaydjian, F. J. *SPEFE*. **1994**, Sept. 9, 200.
- (30) Babadagli, T. *J. Pet. Sci. Eng.* **1996**, *14*, 197–208.
- (31) Wang, R. MS Thesis, University of Wyoming, Laramie, Wyoming, 1999.
- (32) Standnes, D. C. *Energy Fuels* **2009**, *23*, 2149–2156.
- (33) Anderson, W. J. *Pet. Technol.* **1986**, *38* (11), 1246–1262.
- (34) Handy, L. L. *Pet. Trans. AIME* **1960**, *219*, 75–80.
- (35) Pordel Shahri, M.; Jamialahmadi, M.; Shadizadeh, S. R. *J. Pet. Sci. Eng.* **2012**, *82*, 130–139.
- (36) Reis, J. C.; Cil, M. J. *Pet. Sci. Eng.* **1993**, *10* (2), 97–107.
- (37) Zhou, D.; Jia, L.; Kamath, J.; Kovscek, A. R. *J. Pet. Sci. Eng.* **2002**, *33* (1–3), 61–74.
- (38) Tavassoli, Z.; Zimmerman, R.; Blunt, M. J. *Transp. Porous Media* **2005**, *58* (1), 173–189.
- (39) Tavassoli, Z.; Zimmerman, R. W.; Blunt, M. J. *J. Pet. Sci. Eng.* **2005**, *48* (1–2), 94–104.
- (40) Li, K.; Horne, R. N. *SPE Reservoir Eval. Eng.* **2006**, *9* (3), 251–258.
- (41) Li, K. J. *Contam. Hydrol.* **2007**, *89*, 218–230.
- (42) Mirzaei-Paibaman, A.; Masihi, M.; Standnes, D. C. *Transp. Porous Media* **2011**, *89*, 1–14, DOI: 10.1007/s11242-011-9751-8.
- (43) Schmid, K. S.; Geiger, S.; Sorbie, K. S. *Water Resour. Res.* **2011**, *47* (2), W02550 DOI: 10.1029/2010WR009686.
- (44) McWhorter, D. B.; Sunada, D. K. *Water Resour. Res.* **1990**, *26* (3), 399–413.
- (45) Schmid, K. S.; Geiger, S. *Water Resour. Res.* **2012**, *48* DOI: 10.1029/2011WR011566.
- (46) Schmid, K. S.; Geiger, S. *J. Pet. Sci. Eng.* **2013**, [Online] DOI: 10.1016/j.petrol.2012.11.015.
- (47) Mirzaei-Paibaman, A.; Masihi, M.; Standnes, D. C. *Energy Fuels* **2011**, *25* (7), 3053–3059, DOI: 10.1021/ef200305q.
- (48) Bear, J. *Dynamics of Fluids in Porous Media*; Dover: New York, 1972.
- (49) Zappoli, B.; Cherrier, R.; Lasseux, D.; Ouazzani, J.; Garrabos, Y. *Condensed Matter - Statistical Mechanics*. eprint arXiv:cond-mat/0601196, 2006.
- (50) El-Amin, M. F.; Salama, A.; Sun, S. *J. Comput. Appl. Math.* **2012**, DOI: 10.1016/j.cam.2012.09.035.
- (51) McWhorter, D. B. Colorado State University Hydrology Paper No. 49, Colorado State University: Fort Collins, CO, May, 1971, 43 p.
- (52) Bourbiaux, B.; Kalaydjian, F. *SPE Res. Eng.* **1990**, *5* (3), 361–368.
- (53) Zhou, X.; Morrow, N. R.; Ma, S. *SPE J.* **2000**, *5* (2), 199–207.
- (54) Valvatne, P. H.; Blunt, M. J. *Water Resour. Res.* **2004**, *40*, W07406 DOI: 10.1029/2003WR002627.